Journal of the European Ceramic Society 22 (2002) 1129–1135

www.elsevier.com/locate/jeurceramsoc

Fracture behaviour of alumina ceramics by biaxial ball-on-3-ball test

Seong Min Jeong, Sung Eun Park, Hong Lim Lee*

Department of Ceramic Engineering, Yonsei University, Seoul 120 749, South Korea

Received 14 September 2000; received in revised form 10 May 2001; accepted 19 May 2001

Abstract

The fracture behaviour of alumina ceramics was studied using a biaxial ball-on-3-ball test. The polished surfaces of the alumina specimens were indented at positions 0, 1, 2 and 3 mm distant from the center of the specimen along a path (A), passing through the middle point between two supporting balls from the center of the specimen, and also along a path (B), passing through the top point of a supporting ball from the center of the specimen. The fracture strength of the indented specimens was measured using the biaxial ball-on-3-ball test. The fracture strength increased with increasing distance of the indented position from the center of the specimen. The fracture strength of the specimen indented along a path (B) was higher than that of the specimen indented along a path (A). It was also found that the fracture was brought about by the tangential stress rather than the radial stress when the indentations were made at points 1 and 2 mm distant from the center of the specimen. The results were in good agreement with the results of finite element analysis.

Keywords: Al_2O_3; Indentation; Mechanical properties; Strength; Test methods

1. Introduction

The fracture strength of brittle ceramics is generally lowered by defects such as flaws, cracks or inclusions, existing in the sintered body.[1] In uniaxial strength measurements such as 3 or 4 point bending tests, the cracks, which are parallel to the tensile direction (parallel to the longitudinal direction) in the bar type specimen, do not lower the fracture strength of the specimen. However, in a biaxial strength measurement, more reliable fracture strength can be measured because cracks existing in the disc type specimen lower the strength, independently of the directions of the crack arrangement. The maximum tensile stress is induced at the bottom center of the specimen in a biaxial strength test so that edge polishing of the specimen is not necessary, whereas it is very important for bar specimens in the uniaxial strength test.[2,3]

The piston-on-3-ball test is a biaxial strength test designated as a standard test method in ASTM.[4] In addition to the piston-on-3-ball test, there are many other biaxial strength test methods such as ball-on-ring, piston-on-ring, ring-on-ring, uniform-pressure-on-disk and ballon-3-ball according to the shapes of the loading and supporting system. Since the biaxial strength test has clear merits, it has been much studied. Batdorf et al., Evans et al. Lamon et al. and Chao et al. have performed statistical analysis of the fracture strength for the structural ceramics under multiaxial stresses.[5–9] Giovan et al. measured the biaxial fracture strength using a ring-on-ring test and compared results with the uniaxial fracture strength obtained using a 4 point bending test.[10] Shetty et al. studied the biaxial fracture behaviour of ceramics using a ballon-ring test, a piston-on-3-ball test and a ring-on-ring[11,12] The authors measured the biaxial fracture strength of alumina and analyzed the stress distribution for the biaxial strength test using FEM(finite element method).[3]

Because ceramics are brittle, even small flaws on the surface remarkably decrease the fracture strength. Therefore, there have been many studies of fracture caused by initial cracks or surface defects. Lee et al. introduced notches as the initial cracks and studied the effect of the notch size on fracture behaviour.[13] Meschke et al. introduced crack-like voids in AAl_2O_3 and AAl_2O_3–SiC composites and studied the dynamic fracture behaviour using a 4 point bending test.[14] Marshall et al. made indentations on soda-lime glass and studied the variation of the residual strength as a function of the indentation loading.[15]

* Corresponding author. Tel.: +82-2-361-2849; fax: +82-2-312-7735.

E-mail address: htm@yonsei.ac.kr (H.L. Lee).

0955-2219/02/$ - see front matter
PII: S0955-2219(01)00430-7

In this study, considering that specimens are generally hard to contact perfectly between the loading and the supporting modules of most multiaxial systems, the ball-on-3-ball test was adopted. Because the loading and supporting points are all spherical balls in the ball-on-3-ball test, the specimens can be contacted perfectly between the balls of the measuring jig. To investigate the fracture behaviour as a function of the initial crack distance from the center of the specimen, a indents were introduced at positions away from the center of the specimen using a diamond indenter. The experimental results were compared with theoretical results obtained by stress analysis by FEM.

2. Experimental procedure

The alumina specimens for this work were prepared from commercial alumina powder (AES 11, Sumitomo, Japan). The powder was pressed into discs of 20 mm diameter, which were isostatically pressed at 20,000 psi and sintered at 1600 °C for 1 h. The sintered specimens were polished to get a mirror surface with a diamond suspension of particles of 1 μm in diameter, using an autopolisher (LaboPol-5, Struers, Denmark). These specimens were indented at selected positions of the specimen surfaces using a hardness tester (Buehler 1900–2000, HV method) under a load of 10 kg, with a downspeed of 70 μm/s and a loading time of 10 s.

The notations for the indented positions on the surface of the specimen are given in Fig. 1.

The biaxial fracture strength of the alumina disc type specimens was measured by a universal testing machine (H 10K-C, Hounsfield Test Equipment, UK) using a ball-on-3-ball fixture consisting of one loading ball of 5 mm diameter fixed at the center of the specimen and 3 supporting balls of 2 mm diameter, equally separated by 120° on the circle of 12 mm diameter beneath the specimen. The crosshead speed was 0.14 mm/min for a thickness of 2.23 mm of the disc type specimen as designated in ASTM.[4] The Weibull modulus was obtained from the plot of the measured biaxial fracture strength.

3. Results and discussion

3.1. Fracture strength and Weibull modulus before and after indentation

Fig. 2 shows Weibull plots for the disc type specimens which were not indented (NI) and also for those indented at the center of the specimens (CT). The average biaxial strength and Weibull modulus of the NI specimens were 442 and 7.0 MPa, respectively. The average biaxial strength and Weibull modulus of the CT specimens were 173 and 17.4 MPa, respectively. The average indent size was 281.1 μm. The fracture strength and

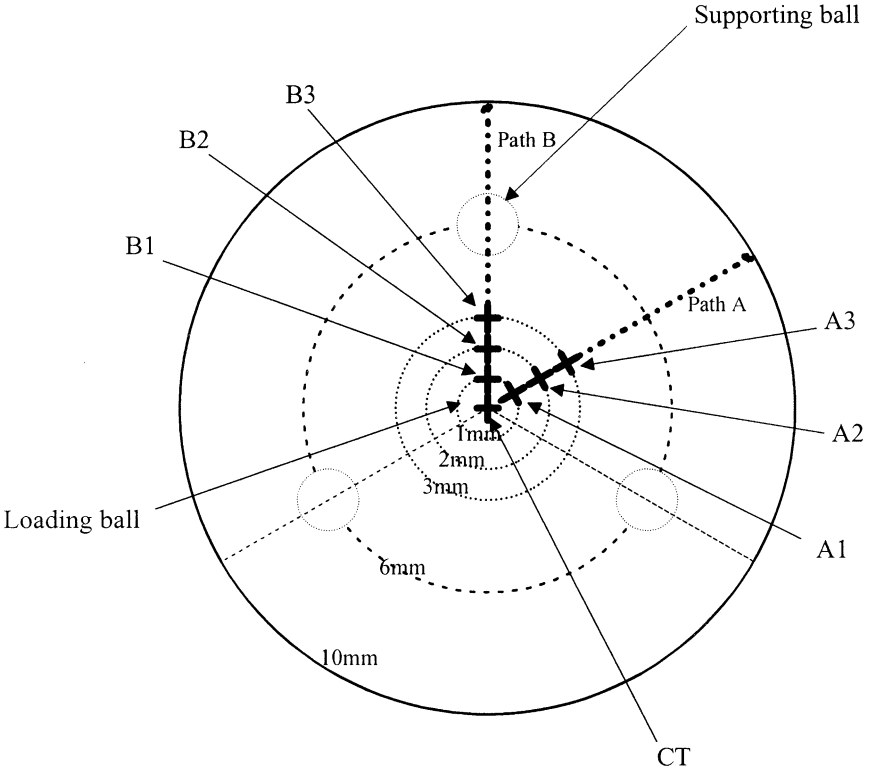

Fig. 1. Schematic diagram of the indented specimen. Al. A2, A3 : indented positions at 1, 2 and 3 mm apart from the center of the specimen along path A. Bl, B2, B3 : indented positions at 1, 2 and 3 mm apart from the center of the specimen along path B.

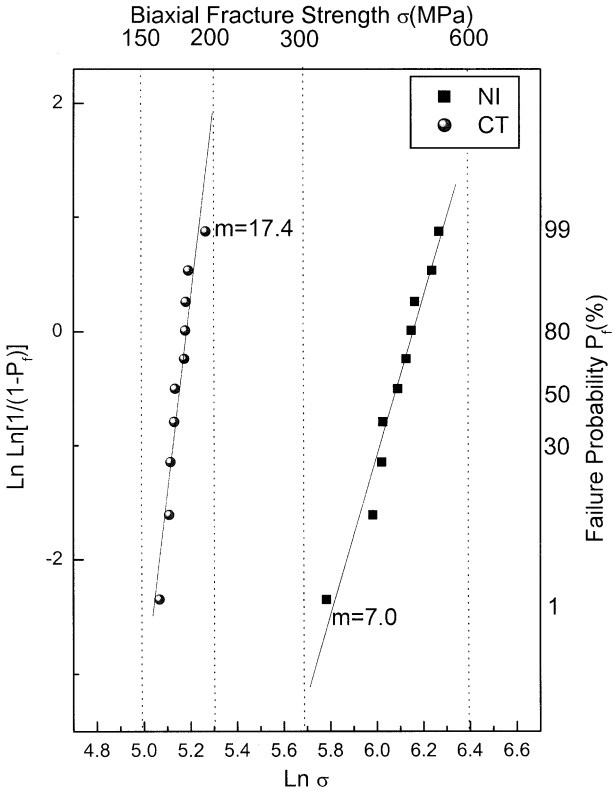

Fig. 2. Weibull plots for the indented and unindented alumina specimens.

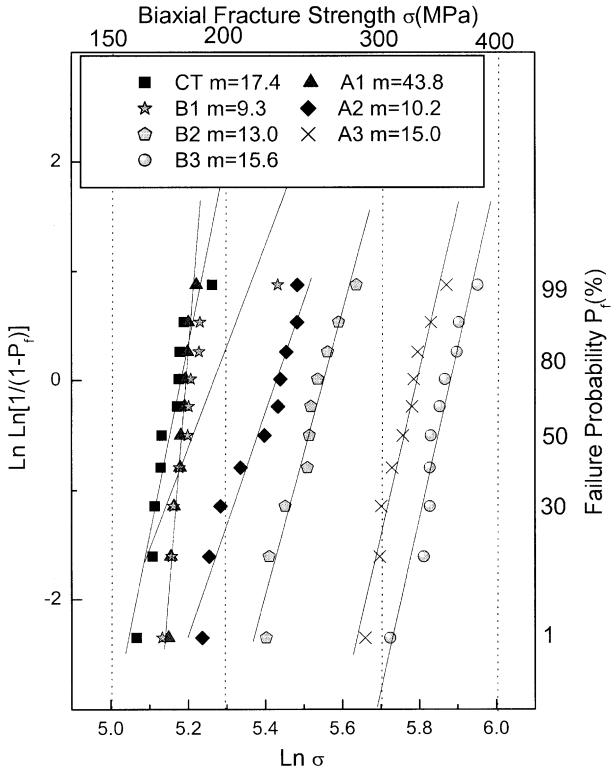

Fig. 3. Weibull plots for the indented alumina specimens (CT, Al, BI, A2, B2, A3, B3).

damage have the relation as the following expression (1)[16]

$$K_{IC} = \sigma_f Y \sqrt{a_f} \quad (1)$$

where K_{IC} is the fracture toughness, σ_f the fracture strength, Y the geometric factor and a_f the length of the crack. The geometric factor Y calculated by expression (1) was 1.348.

3.2. Biaxial fracture strength as a function of distance and direction to the indented positions from the center of the specimen

Fig. 3 shows Weibull plots of biaxial fracture strength of the indented specimens according to the distance to the indented positions and the direction from the center of the specimen. The Weibull moduli of the specimens Al, A2 and A3, the indents of which lie 1, 2 and 3 mm distant from the center of the specimen along path A, passing through the middle point between two supporting balls, were 43.8, 10.2 and 15.0, respectively, as can be seen in Fig. 3.

The Weibull moduli of the specimens B1, B2 and B3, the indents of which lie 1, 2 and 3 mm away from the center of the specimen along path B, passing through the top point of a supporting ball, were 9.3, 13.0 and 15.6, respectively, as can be seen in Fig. 3. The Weibull moduli of all indented specimens were larger than that for NI specimens. However, it was not possible to find any clear correlation between the Weibull modulus and the distance to the indented position or the direction from the center of the specimen.

To investigate the biaxial fracture strength in detail as a function of distance to the indented position from the center of the specimen and also as a function of direction, the fracture strength data shown in Fig. 3 were represented as a box chart in Fig. 4. The average biaxial fracture strength of the specimens indented at the center of the specimen (CT) was 173 MPa. The average biaxial fracture strength values of the specimens Al, A2 and A3 were 178, 218 and 318 MPa, respectively, as can be seen in Fig. 4. The average biaxial fracture strength values of the specimens B1, B2 and B3 were 184, 249 and 348 MPa, respectively, as can be seen in Fig. 4.

The value of the biaxial fracture strength increased with increasing distance to the indented position from the center of the specimen for both paths. The biaxial fracture strength of the specimens indented along path A showed lower values than those of the specimens indented along path B for the same indented distances.

To explore the variation of the biaxial fracture strength, the stress distributions of the specimen under the biaxial ball-on-3-ball loading system were analyzed using the ANSYS FEM package.[17]

The computer simulation model was for 1/6 of the whole system and the model was meshed as shown in Fig. 5.

Table 1 shows the properties of the alumina specimens used in this study. The elastic modulus and Poisson's ratio of the engineering steel used for the loading balls and three supporting balls were 210 and 0.285 GPa, respectively.[18] The alumina specimen module for simulation was meshed with brick elements, and the loading and the supporting ball modules were meshed with tetrahedral elements, as shown in Fig. 5.

Considering the area derived from contacting of the specimen with the balls, contact elements were used for the meshing. The friction coefficient between the alumina specimen and both the loading and supporting balls was taken as 0.4.[19] The numbers of elements and nodes used for meshing the model were 2754 and 3493, respectively.

As the initial condition, the displacement of the lower flat face of the supporting hemisphere was set to zero under loading. Since only 1/6 of the entire model was simulated as shown in Fig. 5. the side views of the loading and supporting balls and also the specimen cut from the entire system shown in Fig. 5 were symmetric for use as the boundary condition for this simulation.

As the loading condition, the maximum displacement of the upper flat face of the loading hemisphere was set as −0.04 mm to the normal direction. This means that the loading ball may be lowered down to the maximum value of 0.04 mm under loading condition.

Figs. 6 and 7, respectively, show the radial and tangential stress distributions on the lower face of the specimen under the ball-on-3-ball system. The maximum stress at the center of the specimen was set to be 100% and the stress on the area where no stress was loaded was set to be 0%. In Figs. 6 and 7, the contour lines show the lines where the same stress is loaded.

The tangential stress along path B decreases more steeply than that along path A.

Fig. 8 shows the radial and tangential stress distributions according to the distance from the center of the specimen along paths A and B.

At the position of the supporting ball, i.e. 6 mm distant from the center of the specimen, both the radial and the tangential stresses along path B varied critically because large compressive stress was induced in this

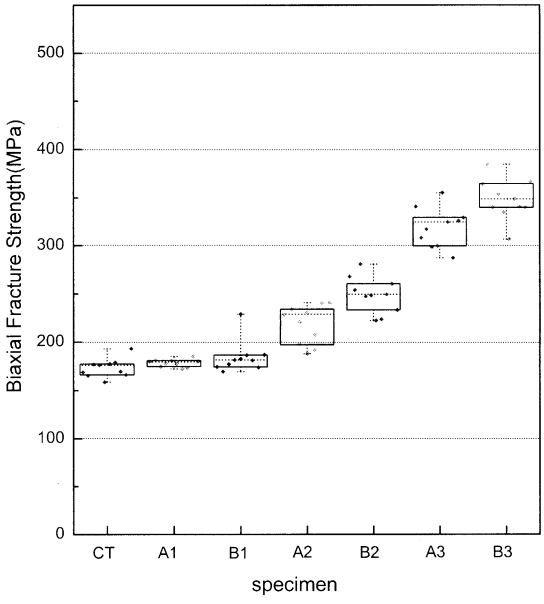

Fig. 4. Fracture strength distribution of alumina ceramics as a function of the indented position.

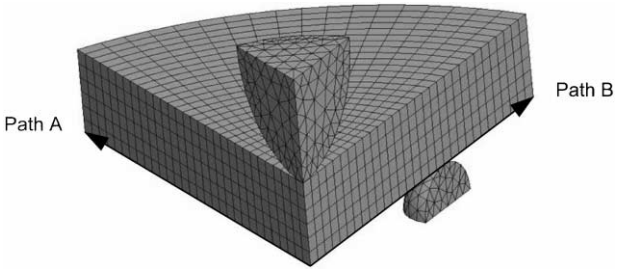

Fig. 5. Finite element meshing used for stress analysis of alumina specimen under the ball-on-3-ball system.

Table 1
Properties of alumina specimens

Four point bending strength	360±23 MPa
Fracture toughness	3.91±0.15 MPa/m^2
Density	3.91±0.01 g/cm^3 (98.2%)
Grain size	2.3 μm
Elastic modulus	330±29 GPa[1]
Poisson's ratio (compression)	0.27[18]
Average thickness	2.23 mm

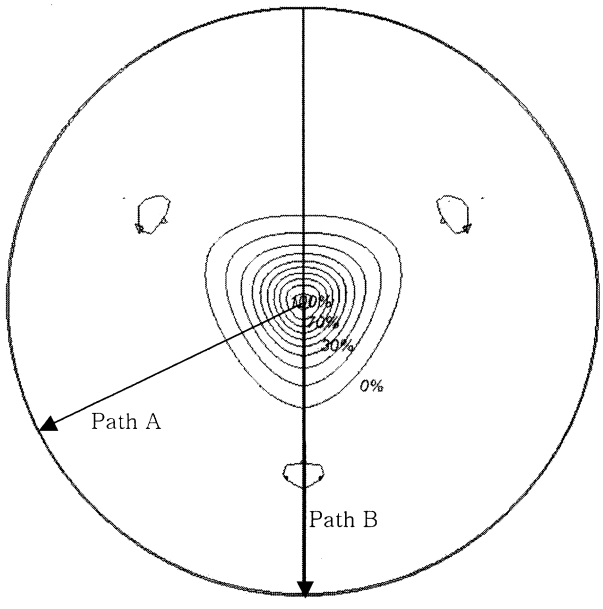

Fig. 6. Radial stress distribution on the lower face of the specimen under the ball-on-3-ball system by the finite element analysis.

region owing to the contact between the specimen and the supporting balls. At the edge of the specimen, only the tangential stress along path A was substantial. This suggests that the fracture of the specimen is caused mainly by the tangential stress.

Actually, as can be seen in Figs. 3 and 4, the biaxial fracture strength values increased with increasing distance to the indented position from the center of the specimen. Moreover, the strength at the same distance showed a higher value for path B than for path A. The stress analysis is in good agreement with the data of Fig. 4.

Fig. 9 shows the calculated geometric factors of indented specimens as functions of distance and direction using expression (1). While the geometric factor of this specimen was theoretically calculated as 1.789 in this study using an equation for 3 point bending test, [21] the experimental values of the specimens CT, Al, A2 and A3 along path A were obtained as 1.348, 1.347, 1.077 and 0.753, respectively. The experimental values of the specimens CT, Bi, B2 and B3 along path A were obtained as 1.348, 1.308, 0.964 and 0.673, respectively. Since K_{IC} is a material constant value and a_f was measured as almost a constant value, geometric factor, Y decreases with increasing the fracture strength of the specimen. The theoretical geometric factors for the specimens indented by Vickers indenter in ball-on-3-ball testing are not available because of the complicated shapes of the indentation for the specimens and also because of the complicated stress distributions of the disc type specimens under for ball-on-3-ball testing.

3.3. The fracture behaviour along indentation distance and direction

Fig. 10(a) and (b) shows the biaxial fracture behaviour of an Ni specimen and a CT specimen, respectively. All three cracks in Fig. 10(a) propagated along path A as expected from the stress shown in Fig. 8.

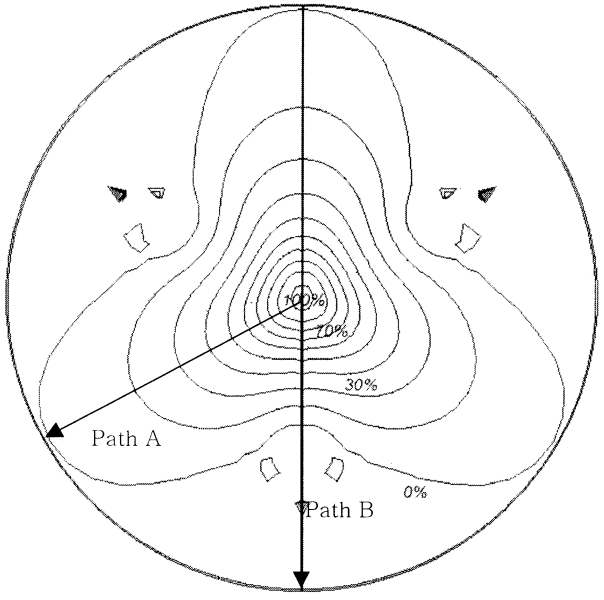

Fig. 7. Tangential stress distribution on the lower face of the specimen under the ball-on-3-ball system by the finite element analysis.

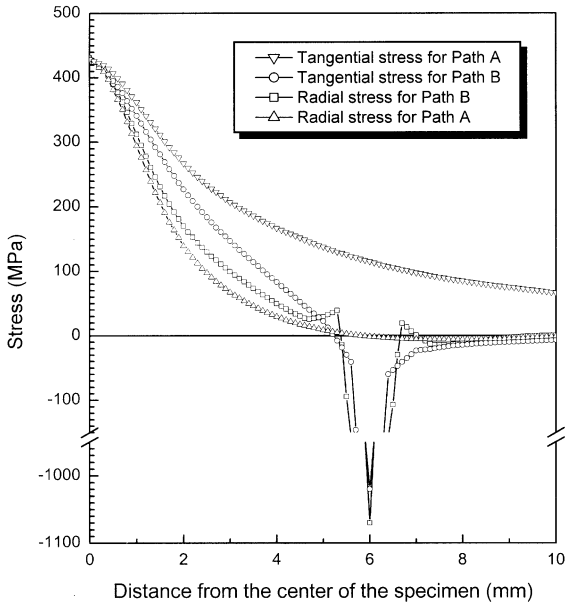

Fig. 8. Stress distribution on the lower face of the specimen under the ball-on-3-ball system.

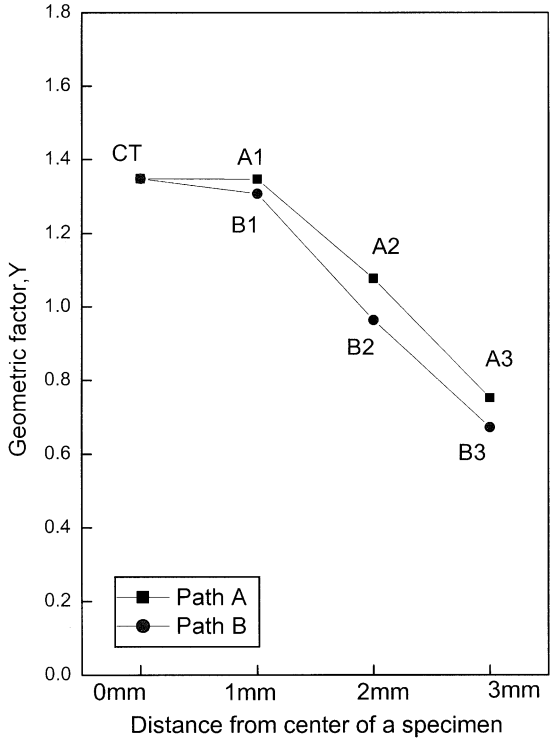

Fig. 9. Calculated geometric factors for the indented alumina specimens.(CT,Al, B1,A2,B2,A3,B3.)

However, in Fig. 10(b) it can be seen that one crack initiated at the indented center of the specimen propagated along path A but that another propagated from the indent toward a supporting ball along path B.

Fig. 11 shows the biaxial fracture behaviour of a specimen indented at 1 mm away from the center of the disc. One indentation was made at 1 mm away from the center along path A (A1) as shown in Fig. 11(a) and the other was made at 1mm away from the center along path B (B1) as shown in Fig. 11(b), however, the cracks were initiated not at the center of the specimen but at the indented position, as shown in Fig. 10. Both indentations (A1 and B1) gave the same result.

Fig. 12 shows the biaxial fracture behaviour of the specimen indented at 2mm away from the center of the disc specimen under the biaxial ball-on-3-ball system. Indentations were made at 2mm away from the center along path A (A2) as shown in Fig. 12(a) and also along path B (B2) as shown in Fig. 12(b), however, the cracks

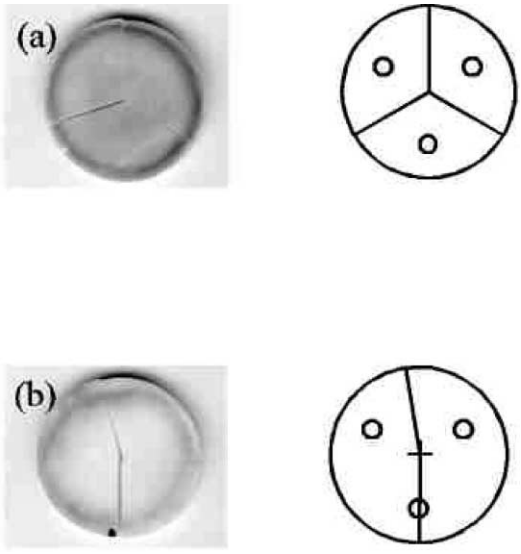

Fig. 10. Fracture morphology of the alumina specimen (a) not indented (NI) and (b) indented at the center (CT).

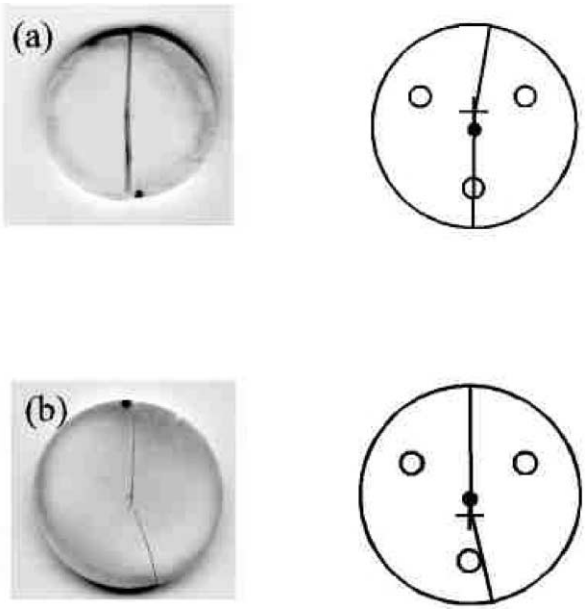

Fig. 11. Fracture morphology of the alumina specimen indented at 1 mm apart from the center of the specimen (a) along path A(Al) and (b) along path B (BI).

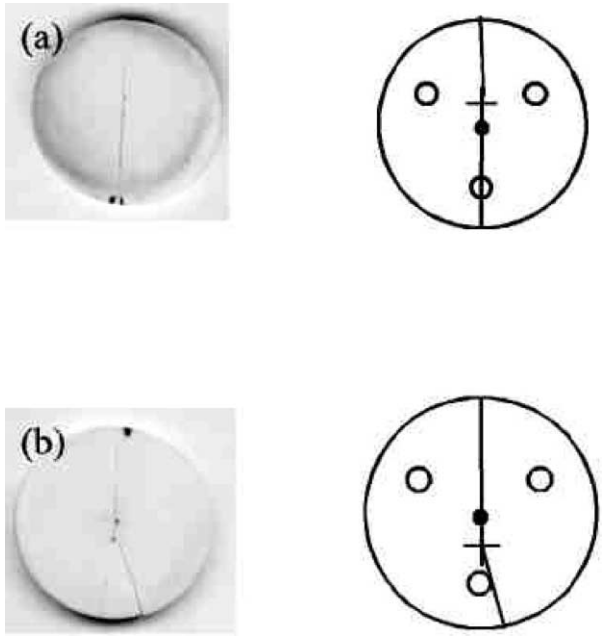

Fig. 12. Fracture morphology of the alumina specimen indented at 2 mm apart from the center of the specimen (a) along path A (A2) and

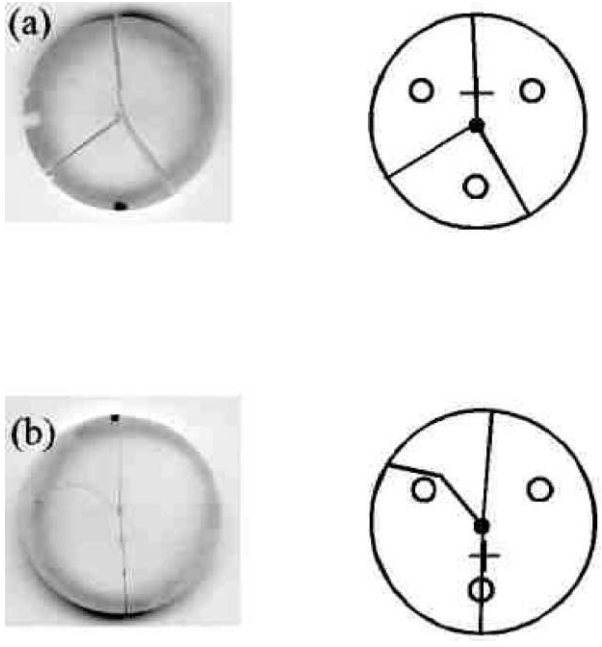

Fig. 13. Fracture morphology of the alumina specimen indented at 3 mm apart from the center of the specimen (a) along path A (A3) and (b) along path B (B3).

were initiated not at the center of the specimen but at the indented position, as shown in Fig. 12. Fig. 12 showed almost the same fracture behaviour as shown in Fig. 11.

Fig. 13 shows the biaxial fracture behaviour of the specimen indented at 3mm from the center of the disc specimen under the biaxial ball-on-3-ball system. Indentation was made 3mm from the center of the specimen along path A (A3) as shown in Fig. 13(a) and along path B (B3) as shown in Fig. 13(b). However, the cracks were initiated not at the indented position but at the center of the specimen.

4. Conclusions

The biaxial fracture behaviour of alumina ceramics was studied using a ball-on-3-ball test and compared with the computer simulation.

The fracture strength increased with increasing distance to the indented position from the center of the specimen. The biaxial fracture strength of the specimen which was indented along path B was higher than that of the specimen which was indented along path A. It was also found that the fracture was brought about by the tangential stress rather than the radial stress. This fracture behaviour was in good agreement with the simulation results by FEM analysis.

When the fracture behaviour of the indented specimen was observed, it was found that the indentations made up to 2 mm from the center of the specimen affected the initiation and propagation of the cracks.

Acknowledgements

This work was supported in part by the Korea Science and Engineering Foundation through the Ceramic Processing Research Center (CPRC) at Hanyang University.

References

1. Mencik, J., *Strength and Fracture of Glass and Ceramics*. Elsevier, Amsterdam, 1992 (pp. 40).
2. Marshall, D. B., An improved biaxial flexure test for ceramics. *Ceramic Bulletin*, 1980, **59**, 551–553.
3. Park, S. E., Lee, J. H. and Lee, H. L., Determination of the biaxial strength by ball-on-3-ball test. *J. Kor. Ceram. Soc.*, 1999, **36**, 225–230.
4. ASTM Standard F394-78, *STM Annual Book of Standards*, Vol. 15.02, Section 16. American Society for Testing and Materials, Philadelphia, PA, 1996, pp. 466–490.
5. Batdorf, S. B., Some approximate treatments of fracture statistics for polyaxial tension. *Int. J. Fract.*, 1977, **13**, 5–11.
6. Evans, A. G., A general approach for the statistical analysis of multiaxial fracture. *J. Am. Ceram. Soc.*, 1978, **61**, 302–303.
7. Lamon, J., Ceramics reliability; statistical analysis of multiaxial failure using the Weibull approach and the multiaxial elemental strength model. *J. Am. Ceram. Soc.*, 1990, **73**, 2204–2212.
8. Chao, L. and Shetty, D. K., Equivalence of physically based statistical fracture theories for reliability analysis of ceramics in multiaxial loading. *J. Am. Cerain. Soc.*, 1990, **73**, 1917–1921.
9. Chao, L. and Shetty, D. K., Reliability analysis of structural ceramics subjected to biaxial flexure. *J. Am. Ceramn. Soc.*, 1991, **74**, 333–344.
10. Giovan, M. N. and Sines, G., Biaxial and uniaxial data for statistical comparisons of a ceramic's strength. *J. Am. Ceram. Soc.*, 1979, **62**, 510–515.
11. Shetty, D. K., Rosenfield, A. R., Bansal, G. K. and Duckworth, W. H., Biaxial fracture studies of a glass-ceramics. *J. Am. Ceram. Soc.*, 1981, **64**, 1–4.
12. Shetty, D. K., Rosenfield, A. R., McGuire, P., Bansal, G. K. and Duckworth, W. H., Biaxial flexure tests for ceramics. *Ceramic Bulletin*, 1980, **59**, 1193–1197.
13. Lee, H. L., Lee, K. H. and Park, S. E., Dynamic fatigue behavior of alumina ceramics. *J Ko, Ceram. Soc.*, 1997, **34**, 1053–1059.
14. Meschke, F., Alves-Riccardo, P., Schneider, G. A. and Claussen, N., Failure behavior of alumina and alumina/silicon carbide nanocomposites with natural and artificial flaws. *J. Mater Res.*, 1997, **12**, 3307–3315.
15. Marshall, D. B. and Lawn, B. R., Flaw characteristics in dynamic fatigue: the influence of residual contact stresses. *J. Am. Ceram. Soc.*, 1980, **63**, 532–536.
16. Mencik, J., *Strength and Fracture of Glass and Ceramics*. Elsevier, Amsterdam, 1992 p. 103.
17. Swanson, J. A., *ANSYS-Engineering Analysis System User's Manual*. Swanson Analysis System. Houston, TX, 15342.
18. Harvey, P. D., *Engineering Properties of Steel*. American Society for Metals, OH, 1982.
19. Melander, A., A finite element study of conditions for early crack growth at inclusions in contact fatigue. *Proceedings of the Sixth International Fatigue Congress*, 1996, **2**, 1081–1086.
20. Brown, W. F. and Srawley, J. E., Plane strain crack toughness testing of high strength metallic materials. *ASTM Spec. Techn. Pub.*, 410, 1967.